FEBS Letters 581 (2007) 2919–2928

The trichomonad cysteine proteinase TVCP4 transcript contains an iron-responsive element

Eduardo Solano-González[a], Eduviges Burrola-Barraza[b], Claudia León-Sicairos[b], Leticia Avila-González[b], Lorena Gutiérrez-Escolano[b], Jaime Ortega-López[a], Rossana Arroyo[b,*]

[a] *Department of Biotechnology and Bioengineering, Centro de Investigación y Estudios Avanzados del IPN (CINVESTAV-IPN), Av. IPN # 2508, Col. San Pedro Zacatenco, CP 07360, Mexico City, Mexico*

[b] *Department of Experimental Pathology, Centro de Investigación y Estudios Avanzados del IPN (CINVESTAV-IPN), Av. IPN # 2508, Col. San Pedro Zacatenco, CP 07360, Mexico City, Mexico*

Received 19 April 2007; revised 17 May 2007; accepted 18 May 2007

Available online 29 May 2007

Edited by Stuart Ferguson

Abstract The differential expression of the *Trichomonas vaginalis* cysteine proteinase TVCP4 by iron at the protein synthesis level and the prediction of an iron-responsive element (IRE)-like stem-loop structure at the 5′-region of the *T. vaginalis* cysteine proteinase 4 gene (*tvcp4*) mRNA suggest a post-transcriptional mechanism of iron regulation in trichomonads mediated by an IRE/IRP-like system. Gel-shifting, UV cross-linking and competition experiments demonstrated that this IRE-like structure specifically bound to human iron regulatory protein-1. IRP-like cytoplasmic proteins that bound human ferritin IRE sequence transcripts at low-iron conditions were also found in trichomonads. Thus, a post-transcriptional regulatory mechanism by iron for *tvcp4* mediated by IRE/IRP-like interactions was found.

Keywords: Cysteine proteinases; Iron regulation; Iron-responsive elements; RNA-binding proteins; Iron-responsive element/iron regulatory protein system; Post-transcriptional regulation; *Trichomonas vaginalis*

1. Introduction

Iron is an essential nutrient for growth, metabolism, and virulence of parasitic protozoa including *Trichomonas vaginalis* [1]. The environment of the human vagina, especially its nutrient and iron concentration, is constantly changing throughout the menstrual cycle. *T. vaginalis* may respond to varying iron concentrations by differential gene expression regulation through a poorly understood mechanism in order to survive, grow and colonize the vaginal hostile environment.

Iron regulates the enhanced expression of some hydrogenosomal proteins [2], phosphohydrolases [3], and virulence genes encoding the trichomonad adhesins AP65 (decarboxylating malic enzyme), AP51 (β-Succinyl Coenzyme A synthetase, SCS), AP33 (α-SCS), and AP120 (pyruvate:ferredoxin oxidoreductase) [4–7]. High-iron concentrations also induce *T. vaginalis* resistance to complement lysis through expression of proteinases that degrade the C3b component [8]. In contrast, transcription of the *T. vaginalis* cysteine proteinase 12 gene (*tvcp12*), and the *flp-1* and *flp-2* genes of fibronectin-like proteins are downregulated by iron [9,10], as well as the expression of the *tvcp65* gene, which negatively affects trichomonal cytotoxicity (our unpublished data).

An iron-responsive promoter and other regulatory elements in the 5′-upstream region of the *ap65-1* gene were identified as a mechanism for positive transcriptional regulation of trichomonad genes by iron [11–13]. However, up to now, this iron-responsive promoter has not been found in other gene sequences coding iron-regulated proteins. Thus, it is likely that other iron regulatory mechanisms may exist in this parasite, possibly at the post-transcriptional level, like the one that mediates the coordinated regulation of key proteins of iron metabolism, such as ferritin, transferrin receptor and erythroid 5-aminolevulinic acid synthase [14,15]. This post-transcriptional mechanism involves an interaction between *trans*-acting cytoplasmic iron regulatory proteins (IRP-1 and IRP-2), and *cis*-acting iron-responsive elements (IREs) present within the 5′- or 3′-untranslated regions (UTR's) of some mRNAs, the IRE/IRP system. Binding of IRE by IRP could inhibit mRNA translation or degradation, depending on the 5′- or 3′-UTR's location [14–17].

T. vaginalis contains many cysteine proteinases (CPs) [18]. Some CPs participate in virulence, such as CP30 and CP62, involved in trichomonal cytoadherence [19–21]; whereas, CP65 and CP39 participate in trichomonal cytotoxicity [22,23]. Furthermore, expression and proteolytic activity of several trichomonad CPs are modulated by iron, especially at the ∼25- to 35-kDa region [10].

In the present study, we found that expression of the cysteine proteinase TVCP4 is upregulated by iron at the post-transcriptional level probably through an IRE/IRP-like system, as in other organisms. To test this hypothesis, binding of an IRE-like hairpin secondary structure of the *tvcp4* mRNA to human IRP proteins, as well as presence of trichomonad IRP-like cytoplasmic proteins, which bind to human ferritin IRE sequence (IRE-fer) transcript, is shown. Information derived from this study will be useful for further elucidating alternative

*Corresponding author. Fax: +52 55 5061 3800x5625.
E-mail address: rarroyo@cinvestav.mx (R. Arroyo).

Abbreviations: CPs, cysteine proteinases; hIRP-1, human iron regulatory protein 1; IRE, iron-responsive element; IRE-fer, human ferritin IRE sequence; ORF, open reading frame; RPCs, RNA–protein complexes; SDS–PAGE, sodium dodecyl sulfate–polyacrylamide gel electrophoresis; *tvcp4*, *Trichomonas vaginalis* cysteine proteinase 4 gene; TYM, trypticase-yeast extract maltose; UNAM, Universidad Nacional Autónoma de México; UTR's, untranslated regions

0014-5793/$32.00
doi:10.1016/j.febslet.2007.05.056

mechanisms of gene expression regulation by iron in *T. vaginalis*.

2. Materials and methods

2.1. Parasites and culture conditions

Trichomonads of *T. vaginalis* isolate CNCD 147 were grown in trypticase-yeast extract-maltose (TYM) medium supplemented with 10% (v/v) heat-inactivated horse serum [24] containing ~20 μM iron [2]. Parasites in the logarithmic growth phase were grown either in iron-rich or in iron-depleted medium by the addition of 250 μM ammonium ferrous sulfate, or 150 μM 2-2′ dipyridyl, an iron-chelator, respectively (Sigma Co., St Louis, MO, USA) into the culture medium [8,9].

2.2. Analysis of tvcp4 gene sequence

The genomic clone 2.9.1.1 [10] with a 3057-bp insert was sequenced (GenBank Accession No. AY679763). This clone contains a 915-bp open reading frame (ORF) encoding a complete CP gene. Its DNA sequence was analyzed by BLAST, WORKBENCH and EXPASY search engines. Locations of DNA transcription-factor binding motifs and predicted RNA secondary structures were analyzed using the *Transfac* program (http://www.gene-regulation.com/pub/programs/alibaba2/index.html) and the *mfold* program (http://bioinfo.rpi.edu/applications/mfold/), respectively [25].

2.3. RT-PCR assays

RT-PCR assays were performed using the Superscript RNase H^- Reverse Transcriptase kit (Stratagene), as recommended by the manufacturer. Total RNA prepared using TRIzol reagent from parasites grown in iron-depleted and iron-rich medium was reverse-transcribed using AMV reverse transcriptase and the oligo (dT) primer. Then, a fragment of 689-bp of the *tvcp4* cDNA was amplified by PCR using as sense primer CP4 5′-GCTAACCTCGGCTTCACA-3′ at position 139–156 nt, and as antisense primer CP4 5′-CCCAGGAGTTACGAACGATC-3′ at position 800–819 nt. A 112-bp fragment of the *T. vaginalis* β-tubulin gene was amplified by PCR with BTUB9 primer: 5′-CATTGATAACGAAGCTCTTTACGAT-3′ and BTUB2 primer: 5′-GCATGTTGTGCCGGACATAACCAT-3′, and used as an internal control [10].

2.4. Western blot analysis

Total trichomonad proteins from 2×10^7 parasites grown in iron-rich and iron-depleted medium obtained as before [26], recombinant human iron regulatory protein (rhIRP-1) [27–29], or HeLa cell cytoplasmic extracts were separated by sodium dodecyl sulfate–polyacrylamide gel electrophoresis (SDS–PAGE) using 10% polyacrylamide gels. Duplicated gels were transferred onto nitrocellulose membrane for Western analysis. Specific proteins were immunodetected with mouse polyclonal antibodies to a synthetic peptide (NAAKGTSWIKS) selected from the most divergent region (residues 188–197) of the TVCP4 proteinase (anti-TVCP4 at 1:12000 dilution), to the recombinant hIRP-1 (anti-IRP antibody at 1:10000 dilution), or to the glutathione-*S*-transferase (GST) portion (anti-GST at 1:10000 dilution) expressed in the pGEX vector (Invitrogen). These sera were prepared in the laboratory using standard techniques [23,30]. As a quantity control, a monoclonal antibody against chicken brain α-tubulin (Zymed) (at 1:100 dilution) was used. Western blots were developed by chemiluminescence using the ECL-Plus kit (Amersham Co., Arlington Heights, IL, USA).

2.5. Purification of recombinant human iron-regulatory protein-1 (hIRP-1)

Recombinant hIRP-1 protein subcloned into pGEX-hIRP plasmid, containing full-length cDNA (kindly donated by Dr. Lucas Kühn), was expressed and purified [27–29]. Purified protein samples were quantified by the Bradford protein assay (Bio-Rad Laboratories, Richmond, CA, USA). Purity of protein samples was assessed by SDS–PAGE on Coomassie brilliant blue-stained gels. Purified rhIRP-1 was used as a control for RNA-band shift, UV-induced cross-linking, and Western blot assays, as well as antigen for polyclonal antibody production in mice (anti-IRP antibody).

2.6. Cytoplasmic extracts from HeLa cells and trichomonad parasites

HeLa cell cytoplasmic extracts were prepared by a modified method [31], and used for gel-shifting and UV cross-linking assays. Briefly, HeLa cells were washed with cold PBS and centrifuged ($2500 \times g$ for 5 min at 4 °C). The cell pellet was suspended in lysis buffer A (10 mM HEPES–NaOH, pH 7.9, 15 mM $MgCl_2$, 10 mM KCl), homogenized in a Dounce homogenizer (45 strokes), and centrifuged ($10000 \times g$ for 30 min at 4 °C). Supernatants were diluted to a final protein concentration of 10 mg/ml and kept at −70 °C.

Trichomonad cytoplasmic extracts were prepared from 1×10^8 trichomonads grown in iron-rich or iron-depleted medium by a modified method [31]. Parasites were lysed by vortexing in 250 μl interaction buffer (10 mM HEPES, pH 7.6, 3 mM $MgCl_2$, 40 mM KCl, 5% glycerol and 0.3% NP-40) containing 7.5 mM TLCK and 1.6 mM leupeptin, incubated for 20 min at 4 °C, and centrifuged at $13000 \times g$ for 5 min at 4 °C. Then, the supernatant was recovered, protein concentration was determined by Bradford (Bio-Rad), and aliquots were kept at −70 °C.

2.7. In vitro transcription of IRE-like sequences

The DNA used for *in vitro* transcription included: pSPT-fer plasmid (a generous gift of Dr. Lucas Kühn) containing human ferritin H-chain IRE (IRE-fer) region, linearized with BamHI [28], three *tvcp4* amplicons, namely, amplicon 31 from bp −3 to 28 (including the *tvcp4* IRE-like hairpin sequence), amplicon 94 from bp −10 to 84 (containing the *tvcp4* IRE-like hairpin sequence), and amplicon 97 from bp 12 to 107 (a *deletion mutant* that disrupts the *tvcp4* IRE-like hairpin sequence). Amplicons were produced by PCR using primers: sense (31): 5′-TAATACGACTCACTATAGGGCACATGTTCGTTCAGGCACCAT-3′, antisense (31): 5′-CTTTCTGCTCATGTGCCTGAACGAACATGTG-3′; sense (94) 5′-TAATACGACTCACTATAGGGATTTCTACACATGTTCGT-3′ and antisense (94) 5′-TCGCCTGTGAACATGTTG-3′; sense (97) 5′- TAATACGACTCACTATAGGGGGCACATGAGCAGAAAGC-3′ and antisense (97) 5′-GGAGAGCCAAATGCCAAG-3′, respectively. PCR sense primers contain a bacteriophage T7 promoter sequence (underline nt) and an additional sequence GG for enhancing transcription. Purified PCR products were used as templates for RNA synthesis using an *in vitro* transcription kit (Promega Corp. Madison, WI, USA). DNA templates and unincorporated nucleotides were removed by DNase RQ1 (Promega) treatment in the presence of RNase inhibitors (Promega) and by gel filtration, respectively. For the synthesis of radiolabeled RNA transcripts, 20 μCi [α^{32}P] UTP (800 Ci/mmol; Dupont) was included in the transcription reaction. An IRE-fer transcript encoding the canonical IRE was used as the positive control. Binding of the 31-, 94-, and 97-nt *tvcp4* transcripts to hIRP-1 was tested by gel-shifting and UV-induced cross-linking assays.

2.8. RNA band-shift assay

RNA–protein complexes were first detected by band-shift assays. ^{32}P labeled RNAs 0.2 ng (2×10^5 cpm) were incubated for 10 min at 25 °C with recombinant hIRP-1 (1 μg/20 μl reaction volume) in the presence of 5 μg heparin, and IRE-IRP complexes were resolved on a 6% non-denaturing polyacrylamide gel and visualized by autoradiography [28].

2.9. UV cross-linking assays

Recombinant hIRP-1 (0.5–1.0 μg), 30 μg cytoplasmic extract of HeLa cells, or 50 μg cytoplasmic extract of *T. vaginalis* were incubated with ^{32}P-labeled RNA probes (5×10^5 cpm) for 20 min at 30 °C in 25 μl reaction mixture containing 10 mM HEPES–KOH, pH 7.4, 3 mM $MgCl_2$, 5% (v/v) glycerol, 1 mM DTT, 100 mM KCl, 40 U RNasin and 6 μg yeast tRNA (Invitrogen Corp., Carlsbad, CA, USA). After RNA-binding, the reaction mixture was placed on ice and irradiated using a UV-lamp (240 nm) for 30 min. Samples were then incubated with RNase A (10 μg) and RNase T1 (20 U) for 30 min at 25 °C. RNA–protein complexes (RPCs) were resolved by SDS–PAGE on a 10% polyacrylamide gel. The gels were stained with Coomassie brilliant blue and dried, and radioactive bands were visualized by autora-

diography [32]. For competition assays, a 10- and 20-fold molar excess of unlabeled 31-nt *tvcp4* IRE-like transcript or IRE-fer RNA were incubated with cytoplasmic extracts for 15 min at 4 °C before the addition of labeled RNA. tRNA was used as a heterologous competitor [32]. Densitometry analysis of cross-linked bands was performed with the Quantity One program (Bio-Rad).

2.10. Immunoprecipitation of IRP-like proteins in the RPCs after UV cross-linking assays with an anti-IRP antibody

RPCs were incubated with 10 μl of protein G-Sepharose 4B beads (pre-equilibrated in lysis buffer A, for 2 h at 4 °C, and centrifuged at 12000 × *g* for 5 min) (Invitrogen) after UV cross-linking and RNase treatment. The supernatants were then incubated with 6.0 μl of mouse polyclonal anti-recombinant hIRP-1 antibody for 18 h at 4 °C. These immunocomplexes were immobilized on protein G-Sepharose beads (30 μl) saturated with 2% bovine serum albumin, for 3 h at 4 °C. Unbound materials were eliminated by washing six times with 10 mM Tris–HCl buffer (pH 8.0), containing 150 mM NaCl, 1% (v/v) NP-40, and 3 mM EDTA. Bound proteins were eluted with Laemmli buffer and analyzed by SDS–PAGE, followed by autoradiography. Parallel reactions were carried out with the pre-immune normal mouse serum as a negative control [32].

3. Results

3.1. The complete T. vaginalis tvcp4 gene encodes a cathepsin L precursor proteinase

Genomic clone *2.9.1.1* (with a 3057-bp insert) contains a 915-bp ORF with an ATG initiation and TAA stop codons, non-coding regions up- and downstream of it containing the Inr promoter [33] and putative polyadenylation regulatory sequences, respectively [34]. The deduced protein (305-aa) is 99% identical to the partial *tvcp4* cDNA sequence reported before [35]. TVCP4 protein corresponds to a putative papain-like precursor proteinase with a predicted molecular mass of 33.8-kDa and a theoretical p*I* of ~7.5. The putative TVCP4 precursor contains a signal peptide (SP, residues 1–25), pre- and pro-regions (residues 26–86), and an ERFNIN-like sequence (white box, residues 26–45). The putative mature TVCP4 protein begins at residue 87 (arrowhead) with a predicted mass of 23.6-kDa and a theoretical p*I* of ~5.22

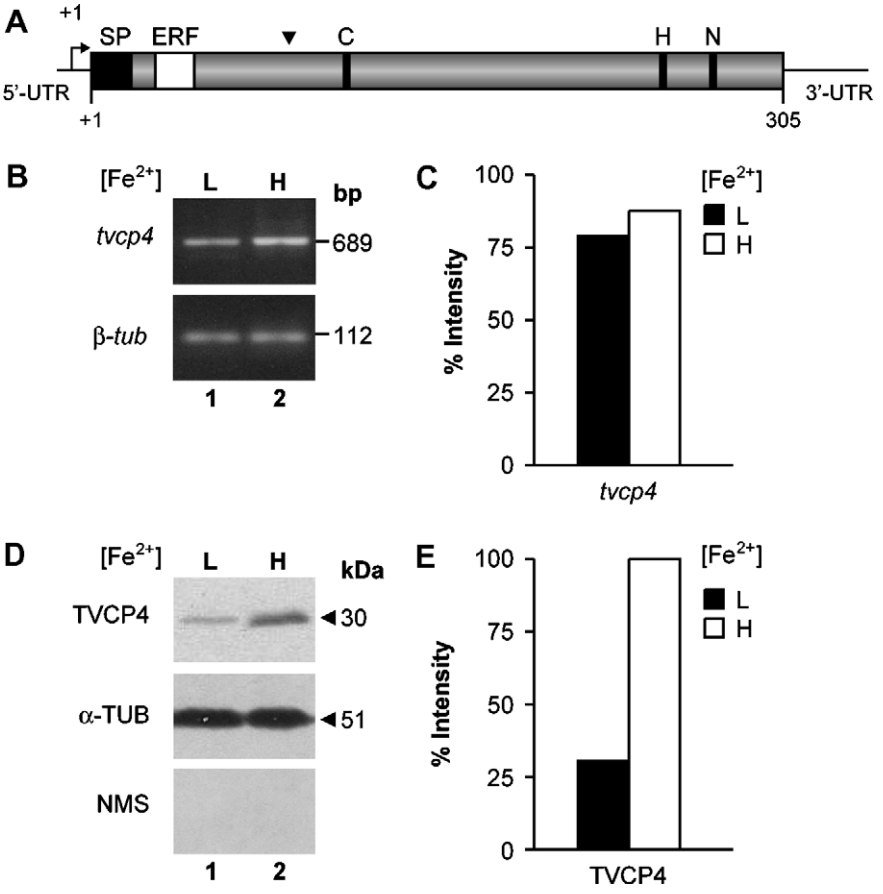

Fig. 1. The complete *T. vaginalis tvcp4* gene and effect of iron on transcription and translation of TVCP4. (A) Principal motifs of the deduced amino acid sequence of the TVCP4 protein, residues forming the putative signal peptide (SP), pre-pro region (small grey box), ERFNIN sequence (ERF, white box), (▼) putative start site of the mature CP, C, H and N, and the amino acid residues (Cys, His and Asp) forming the catalytic triad of the TVCP4 cysteine proteinase. (B) RT-PCR products obtained with specific primers for the *tvcp4* (*tvcp4*), or β-tubulin (β-*tub*) gene using cDNA from parasites grown in: lane 1, iron-depleted (L); or lane 2, iron-rich (H) medium. (C) Densitometric analysis of the RT-PCR products from (B) using the QUANTITY ONE software. The intensity obtained from the β-*tub* product was used as 100%. (D) Western blot analysis using nitrocellulose membranes containing TCA precipitated total protein extracts from: lane 1, parasites grown in iron-depleted (L); or lane 2, iron-rich (H) medium with antibodies against a TVCP4 divergent synthetic peptide (TVCP4; 1:12000 dilution), α-tubulin from chicken brain (ZYMED; 1:100 dilution) (α-TUB) or pre-immune normal mouse serum (NMS; 1:12000 dilution). The last two antibodies were used as a quantity control and as a negative control, respectively. (E) Densitometric analysis of protein bands detected by Western blot from (D) using the QUANTITY ONE software. The band intensity obtained with the anti-TVCP4 over protein extracts from parasites grown in iron-rich medium (H) was used as 100%. Experiments were performed three times with similar results.

(Fig. 1A). It also contains the catalytic triad residues C25, H164, and N183.

3.2. High iron trichomonads have increased amounts of TVCP4

We performed RT-PCR assays using specific primers for *tvcp4*, and RNA from parasites grown in iron-rich and iron-depleted medium. The expected 689-bp product was obtained with RNA from both iron conditions, showing only minor changes (Fig. 1B, *tvcp4*). As an internal control, we obtained identical products of 112-bp for the β-tubulin gene by RT-PCR with RNA from both iron conditions handled identically (part B, β-*tub*), which was used as 100% intensity in the densitometry scans (part C).

We performed Western blot with extracts from high- and low-iron parasites used above, and probed with anti-TVCP4 peptide serum antibody. Fig. 1 (parts D and E) shows 3-fold increased amounts of TVCP4 in iron-rich compared to iron-depleted parasites. As a control, similar amounts of protein were detected with antiserum to α-tubulin in both iron conditions. These data show that iron is without effect on gene transcription and is increasing translation of TVCP4.

3.3. An IRE-like structure is found inside the coding region of the *tvcp4* mRNA

To investigate the mechanism by which amounts of TVCP4 are increased in high-iron parasites, we first analyzed a 1306-bp region of the *tvcp4* 5′-UTR, obtained from the draft *T. vaginalis* genome sequence [36] with the *Transfac* program. Typical regulatory sequences of trichomonad genes at the 5′-UTR, such as the Inr promoter element TCATTT [33] located at 12-nt upstream of the initiation codon ATG, were observed (Fig. 2A). However, none of the reported DNA motifs were related to iron regulation previously described for *ap65-1* gene [11–13]. Thus, we searched for iron regulatory elements (IREs) in the *tvcp4* mRNA that could be involved in a post-transcriptional regulatory mechanism mediated by an IRE/IRP-like system [14–17]. Analysis by the *mfold* program [25] of 21-nt upstream and 107-nt downstream of the ATG codon of *tvcp4* mRNA revealed a sequence with possible formation of stem-loop RNA secondary structures (Fig. 2A). The first 23-nt downstream of the ATG codon formed a stable (ΔG −5.7 kcal/mol) IRE-like stem-loop structure with a 6-nt loop (part B3), a 5-nt upper stem, a bulge, and a 3-nt lower stem [14,28,29].

The predicted 23-nt *tvcp4* IRE-like stem-loop RNA secondary structure was compared with the secondary structures of the human IRE-fer determined by NMR [37] (part B1), and with the IRE present in the mitochondrial 75-kDa subunit of mitochondrial complex I [38] (part B2). The 6-nt loop of the *tvcp4* IRE-like hairpin has a 5′-GGCACA-3′ sequence, although it possesses a G1 and C5 nucleotide arrangement similar to the hairpin loop of IRE-fer mutants that bind to IRP proteins [28,29] and can be therefore classified as a G^1C^5-type IRE element (part C). Even though the five-paired

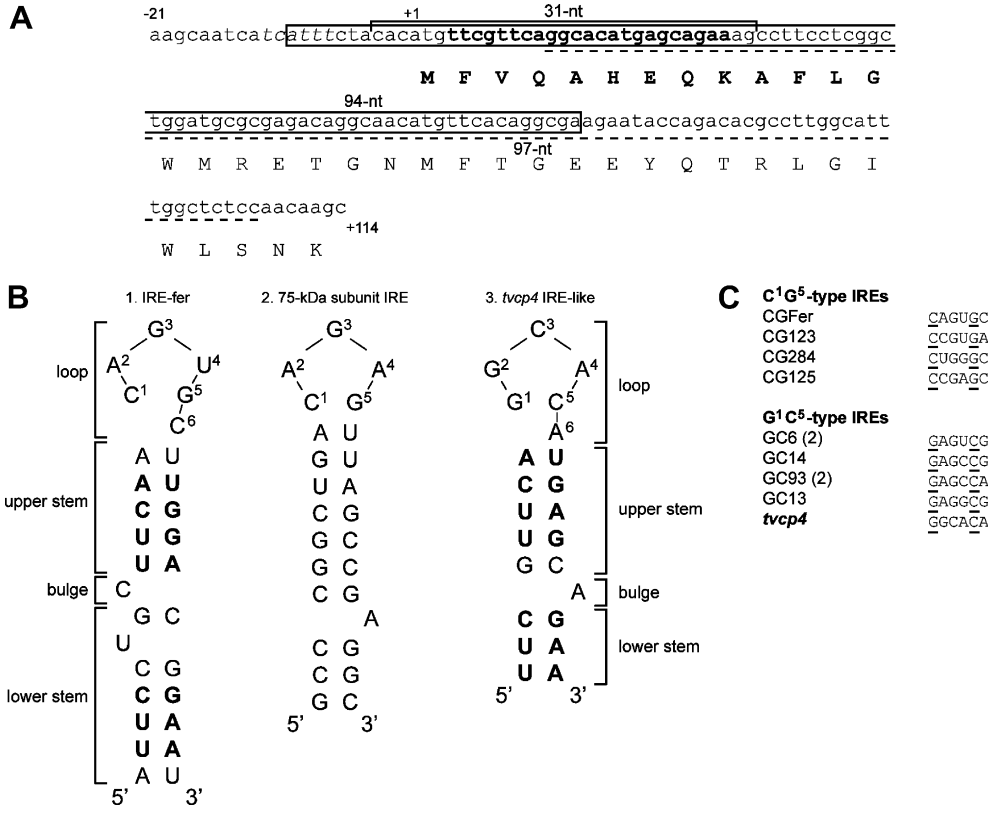

Fig. 2. Proposed *tvcp4* IRE-like hairpin stem-loop structure. (A) Sequence of 136-nt of the 5′-region of the *tvcp4* gene showing the Inr sequence in italics; 31- (brackets), 94- (large box), and 97-nt (dashed line) sequences used for *in vitro* transcription. Boldface letters indicate the 23-nt hairpin sequence. (B) (1) Stem-loop secondary structure of the H-ferritin IRE (IRE-fer) RNA confirmed by NMR; (2) IRE predicted secondary structures of the 75-kDa subunit of the mitochondrial complex I and (3) the *tvcp4* IRE-like mRNAs. (C) Comparison of the *tvcp4* loop sequence with loop sequences of some IRE-fer mutants [29] with C^1G^5 or G^1C^5 arrangement.

nucleotide upper stem of the *tvcp4* IRE-like hairpin is similar to the one present in the IRE-fer [14,15], the *tvcp4* IRE-like structure has a bulge with an A at the 3′-strand as in the 75-kDa subunit of mitochondrial complex I, which is functional [38], instead of a C in the 5′-strand of the IRE-fer hairpin [28,29]. Moreover, the *tvcp4* IRE-like lower stem is three-paired nt similar to the one found in the IRE of the 75-kDa subunit of mitochondrial complex I, while in the IRE-fer it is five-paired nt long. Interestingly, four out of the five-paired nt in the upper stem, and the three-paired nt of the lower stem of the *tvcp4* IRE-like RNA predicted secondary structure are identical to the corresponding IRE-fer sequence (parts B1 and 3, bold letters).

3.4. The tvcp4 IRE-like hairpin structure interacts with the recombinant hIRP-1 and with a ~98-kDa protein band from HeLa cytoplasmic extracts

The ability of *tvcp4* IRE-like hairpin to form RPCs with IRP-like proteins was then tested by gel-shifting and UV cross-linking assays (Fig. 3). We first analyzed the predicted secondary structure of different sized transcripts, 31- (−3 to 28), 94- (−10 to 84), and 97-nt (12–107) from the 5′-end of *tvcp4* for the presence of IRE-like structures (Fig. 3A). Only the 97-nt RNA predicted secondary structure did not form an IRE-like structure. Thus, the 97-nt transcript was used as a *deletion mutant* with a disrupted IRE-like structure.

We next tested by gel-shifting assays using the recombinant hIRP-1 protein the ability of the different *tvcp4* IRE-like transcripts to bind to IRP proteins. Upon incubation with the ^{32}P-labeled 31- and 94-nt *tvcp4* RNA probes, the recombinant hIRP-1 showed a triple band-shift (part B, lanes 3 and 4), as with the control IRE-fer (lane 2); whereas, with the 97-nt deletion mutant *tvcp4* mRNA or free RNA transcripts, used as negative controls, no band-shift was observed (lanes 1 and 5). These data show that only *tvcp4* RNA probes containing the intact IRE-like structure form RNA–protein complexes with the recombinant hIRP-1.

We then performed UV-induced cross-linking assays with the same ^{32}P-labeled *tvcp4* RNA probes and HeLa cytoplasmic extracts, as a source of IRP, to determine the size of the proteins in the RPCs. Fig. 3C shows that 45-kDa and 98-kDa proteins cross-linked with radiolabeled IRE-fer RNA used as a positive control and with the 31- and 94-nt IRE-like *tvcp4* RNA probes (lanes 2, 4, and 6, respectively). In addition, a 60-kDa radioactive band was also observed with the trichomonad transcripts (lanes 4 and 6). Neither the 45-kDa, 60-kDa nor 98-kDa proteins cross-linked with the 97-nt transcript of the *tvcp4* IRE-like deletion mutant (lane 8). A smaller unknown protein band binding the 97-nt transcript may be an unrelated RNA-binding protein present in HeLa cytoplasmic extracts. As expected, no radiolabeled bands (lanes 1, 3, 5, and 7) were observed in mock experiments. These data show

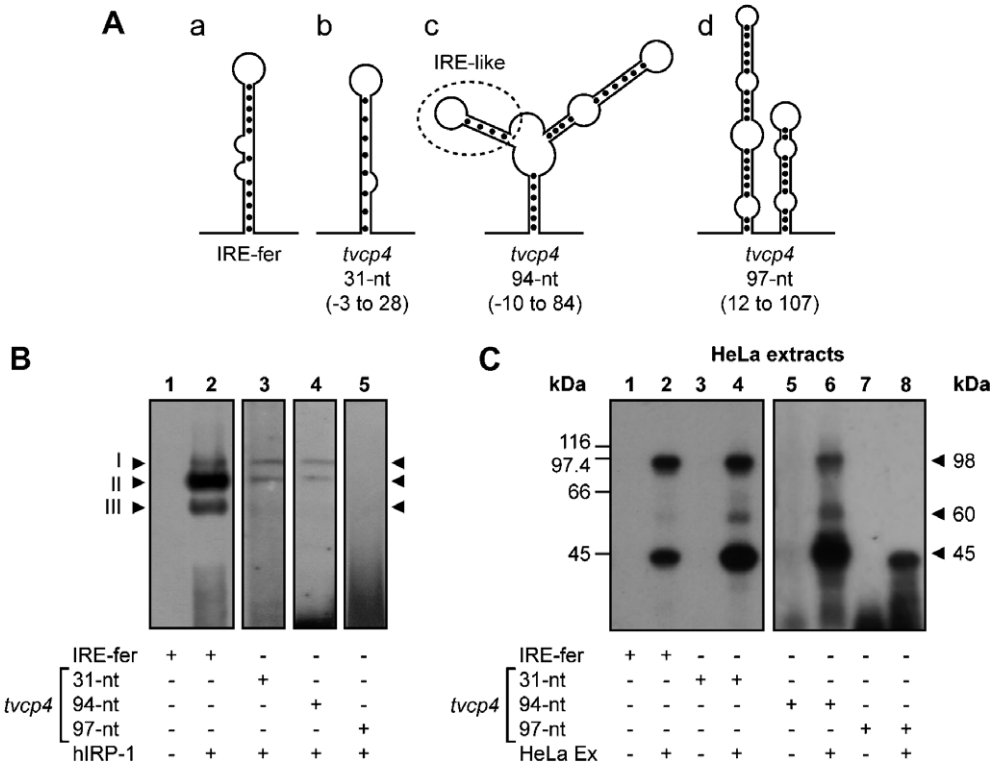

Fig. 3. Proposed stem-loop secondary structures of different transcripts from the 5′-region of the *tvcp4* gene, and detection of RNA–protein complexes by gel-shifting and UV cross-linking assays. (A) Schematic representation and sequence position of secondary structures of: (a) human ferritin IRE (IRE-fer) (positive control) [37]; predicted *tvcp4* IRE-like RNA structures obtained with the *mfold* program: (b) 31-nt (−3 to 28), (c) 94-nt (−10 to 84; dashed circle), and (d) 97-nt (12 to 107) deletion mutant. (B) Gel-shifting, and (C) UV cross-linking of ^{32}P-labeled *tvcp4* transcripts (31-, 94-, and 97-nt) (5×10^5 cpm) to recombinant hIRP-1 (hIRP-1) (B) and HeLa cytoplasmic extracts (HeLa Ex) (C), as described in Section 2. Selected molecular mass markers are indicated in kilodaltons (kDa). Arrowheads indicate position of RNA–protein complex bands I, II or III (B) on native gels; or size of protein bands cross-linked to radioactive RNA transcripts (C) on denaturing gels detected after autoradiography. Experiments were performed three times with similar results.

that the complete 23-nt stem-loop RNA from *tvcp4* is needed for RPC formation with IRP proteins.

3.5. The tvcp4 IRE-like hairpin specifically interacts with an IRP-like protein from HeLa cell extracts

Specificity of RNA–protein binding complexes using the 31-nt IRE-like transcript was demonstrated with UV cross-linking competition assays. We used 10- and 20-fold molar excess of unlabeled homologous 31-nt IRE-like RNA, heterologous IRE-fer RNA, and a non-related tRNA as competitors (Fig. 4A). Unlabeled 31-nt IRE-like RNA partially, up to 79%, and completely competed with homologous labeled RNA (lanes 3 and 8, respectively), as compared to controls without competitor (lanes 2 and 7). On the contrary, unlabeled IRE-fer RNA did not or slightly cross-competed, up to 30%, with the labeled 31-nt IRE-like RNA for specific RPC formation in HeLa cell extracts (lanes 4 and 9). Interestingly, the unlabeled 31-nt transcript, as a heterologous competitor at 10- and 20-fold molar excess (part B), partially, up to 70%, and completely competed with the labeled IRE-fer RNA (lanes 4 and 8) for specific RPC formation, as compared to RPC control (lanes 3 and 7, respectively); whereas, unlabeled homologous IRE-fer RNA partially competed up to 34% and 60% with itself (lanes 5 and 9, respectively), as expected at these molar excesses. An excess of tRNA had no effect on RPCs formation with either RNA probes (part A, lanes 5 and 10; part B, lanes 6 and 10). These data show that the *tvcp4* RNA and HeLa IRP RNA–protein complexes are specific. These results also show that the *tvcp4* IRE-like RNA is a better competitor than the IRE-fer RNA for RPC formation under these experimental conditions. Thus, these data may suggest higher affinity of this unusual IRE-like structure than the IRE-fer RNA for the IRPs present in HeLa cell extracts.

To determine whether the 98-kDa protein observed in the cross-linking experiments using HeLa cell extracts corresponds to the hIRP-1, we performed Western blot assays using

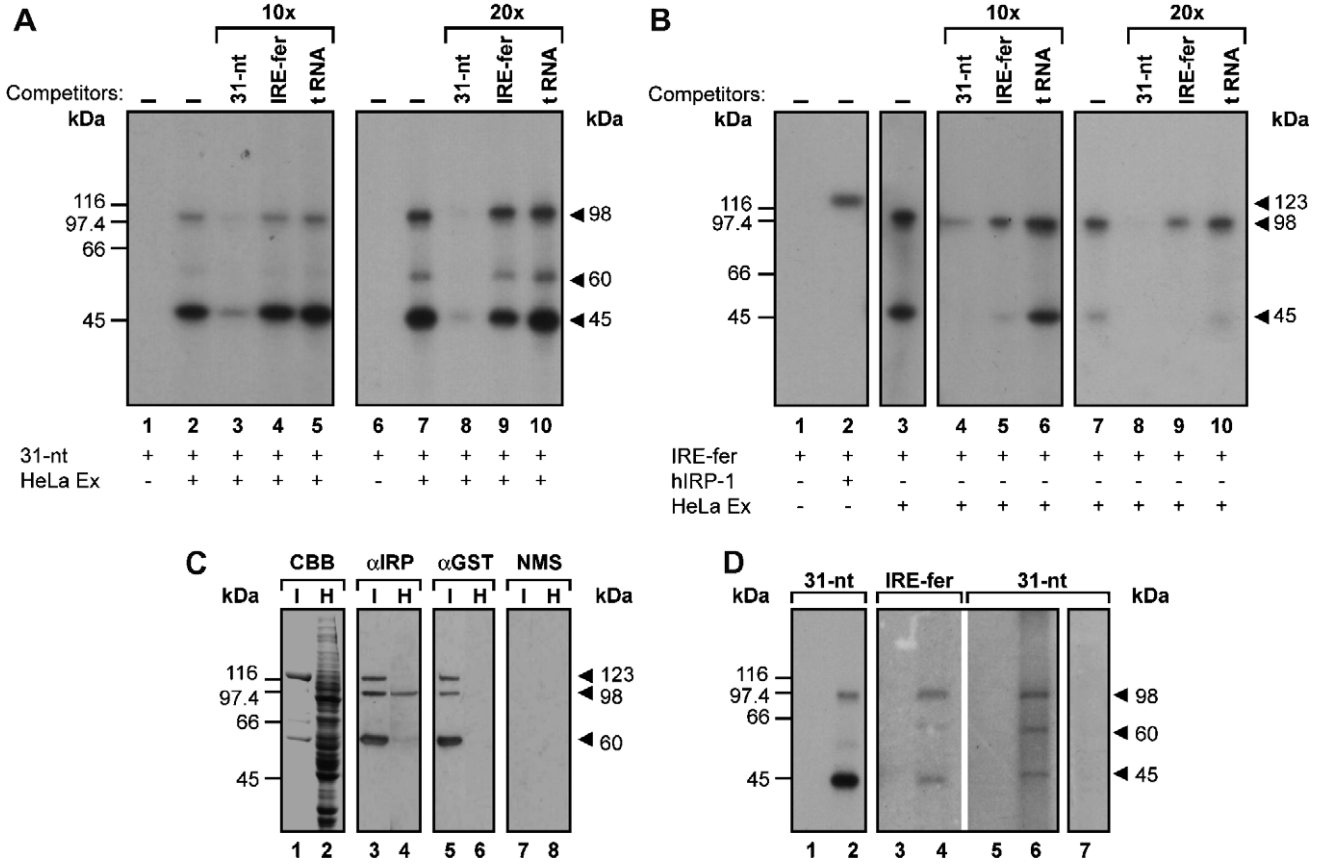

Fig. 4. Specific interaction between the 31-nt *tvcp4* IRE-like structure and iron-regulatory proteins. (A) Specificity of the interaction of the 31-nt *tvcp4* IRE-like RNA to HeLa IRP-1-like protein determined by UV cross-linking competition assays performed in the absence (lanes 2 and 7), or presence of 10- and 20-fold molar excess (10× and 20×, respectively) of unlabeled 31-nt transcript (lanes 3 and 8), or IRE-fer RNA (lanes 4 and 9). The same molar excess of tRNA was used as heterologous competitor (lanes 5 and 10). Mock controls without proteins (lanes 1 and 6) were also used as controls. (B) Similar cross-linking competition assays carried out with the IRE-fer RNA and HeLa cytoplasmic extracts in the absence of competitors (lanes 3 and 7), or in the presence of 10- or 20-fold molar excess (10× and 20×) of unlabeled 31-nt transcript (lanes 4 and 8), IRE-fer RNA (lanes 5 and 9), or tRNA (lanes 6 and 10). Recombinant hIRP-1 binding to IRE-fer RNA (lane 2) was used as a positive control. Mock control without protein (lane 1) was also used as a control. (C) Western blot assays using the anti-recombinant hIRP-1 (α-IRP, lanes 3 and 4), anti-GST (α-GST, lanes 5 and 6), or pre-immune normal mouse (NMS, lanes 7 and 8) serum over nitrocellulose membranes containing hIRP-1 (I; lanes 1, 3, 5, and 7), or HeLa cytoplasmic extracts (H; lanes 2, 4, 6, and 8). Lanes 1 and 2, protein patterns (I and H) stained with Coomassie brilliant blue (CBB). (D) Immunoprecipitation assay of RPCs using the anti-recombinant hIRP-1 (lanes 3–6), or the pre-immune normal mouse (lane 7) serum after UV cross-linking of RNA probes: IRE-fer (lanes 3 and 4), or 31-nt *tvcp4* IRE-like (lanes 5–7) to HeLa cell extracts. Cross-linking controls: free 31-nt IRE-like transcript (lane 1) and RPC of 31-nt IRE-like RNA with HeLa IRP-1 (lane 2). Molecular mass markers are indicated in kilodaltons (kDa). Experiments were performed three times with similar results.

the anti-recombinant hIRP-1 (α-IRP) antibody. The anti-IRP antibody recognized a 98-kDa band in HeLa cell cytoplasmic extracts (part C, lane 4) and three bands of 123-kDa, 98-kDa, and 60-kDa in the enriched recombinant hIRP-1 protein, which was used as a positive control (lane 3). The anti-GST antibody (used as a control) also recognized the three bands of the recombinant hIRP-1 protein (lane 5), but did not react with the HeLa cells extracts (lane 6). As expected, no protein bands were detected by the pre-immune normal mouse serum (NMS) in any of the tested protein samples (lanes 7 and 8).

We performed immunoprecipitation assays of RPCs with the anti-IRP antibody after the UV cross-linking assays with HeLa cytoplasmic extracts (part D, lane 2). The anti-IRP antibody immunoprecipitated proteins of 98-kDa, 60-kDa, and 45-kDa cross-linked to the 31-nt *tvcp4* IRE-like RNA probe (lane 6). Similar immunoprecipitation results were obtained using the RPCs formed with the IRE-fer probe (lane 4) used as a positive control. Pre-immune normal mouse serum (lane 7) and the mock experiment (lanes 3 and 5) with anti-IRP antibody, used as negative controls, did not detect labeled protein bands. These results demonstrate that the 31-nt *tvcp4* IRE-like RNA can interact with a 98-kDa protein band, corresponding to the size of HeLa cells IRP-1. The 60-kDa and 45-kDa proteins immunoprecipitated with the anti-IRP antibody may be part of the hIRP-1 degradation products.

3.6. Presence of IRP-like proteins in T. vaginalis and effect of iron on the RPCs formation

To support our hypothesis of gene expression regulation by iron through a post-transcriptional mechanism mediated by an IRE/IRP-like system in trichomonads, we investigated the presence of IRP-like proteins in *T. vaginalis* cytoplasmic extracts and the effect of iron on RPCs formation. Thus, gel-shifting and cross-linking assays with labeled IRE-fer probe and cytoplasmic extracts of trichomonads grown in iron-rich and iron-depleted medium were performed (Fig. 5). In the gel-shifting assays, two RPC bands were observed with trichomonad extracts from parasites grown in iron-depleted, but not in iron-rich medium (part A, lanes 3 and 4). These complexes showed less mobility than the bands obtained with the rhIRP-1 used as a positive control (lane 2).

We performed UV cross-linking assays using trichomonad cytoplasmic extracts in iron-depleted and iron-rich conditions. A 98-kDa protein cross-linked to radiolabeled IRE-fer RNA was only detected in iron-depleted conditions (part B, lanes 2 and 3). This radioactive band has a similar size to that of the IRP-1 protein from HeLa cells cross-linked to the IRE-fer probe (lane 1), used as a positive control. A 45-kDa radioactive protein was also observed with HeLa extracts (lane 1), probably a degradation product.

4. Discussion

This report shows that synthesis and amounts of the *T. vaginalis* cysteine proteinase TVCP4 increased in the presence of iron. It appears to be regulated by a post-transcriptional iron regulatory mechanism mediated by specific RNA–protein interactions through an IRE/IRP-like system. This type of regulation in this early-branching protozoan is supported by the presence of an iron-responsive element (*tvcp4*) at the 5′-end of the TVCP4 mRNA coding region, and cytoplasmic IRP-like proteins in trichomonads. Interestingly, the TVCP4 IRE structure is located in an unusual place for translational regulation. Rather than being in the *tvcp4* 5′-UTR, it is inside the coding

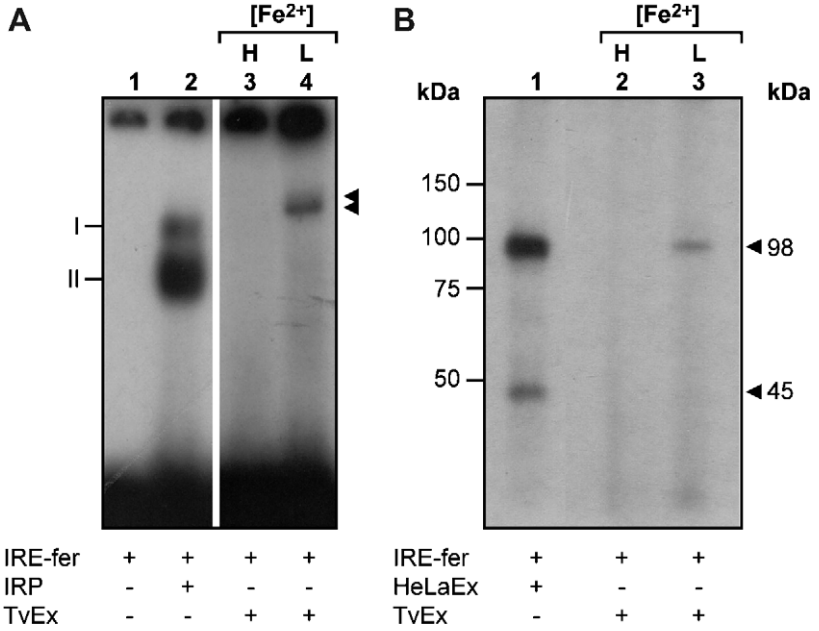

Fig. 5. Presence of IRP-like proteins in *T. vaginalis* and effect of iron on RPC formation. (A) Gel-shifting assays to detect RPC formation between IRE-fer RNA with rhIRP-1 protein, as a positive control (lane 2); IRE-fer RNA with *T. vaginalis* cytoplasmic extracts from parasites grown in iron-rich (H), or iron-depleted (L) medium (lanes 3 and 4). Free IRE-fer RNA, as a negative control (lane 1). (B) Cross-linking assays between IRE-fer RNA and HeLa cell extracts (lane 1), used as a positive control; IRE-fer RNA, and *T. vaginalis* extracts from parasites grown in iron-rich (H), or iron-depleted (L) medium (lanes 2 and 3). Molecular mass markers are indicated in kilodaltons (kDa). Experiments were performed three times with similar results.

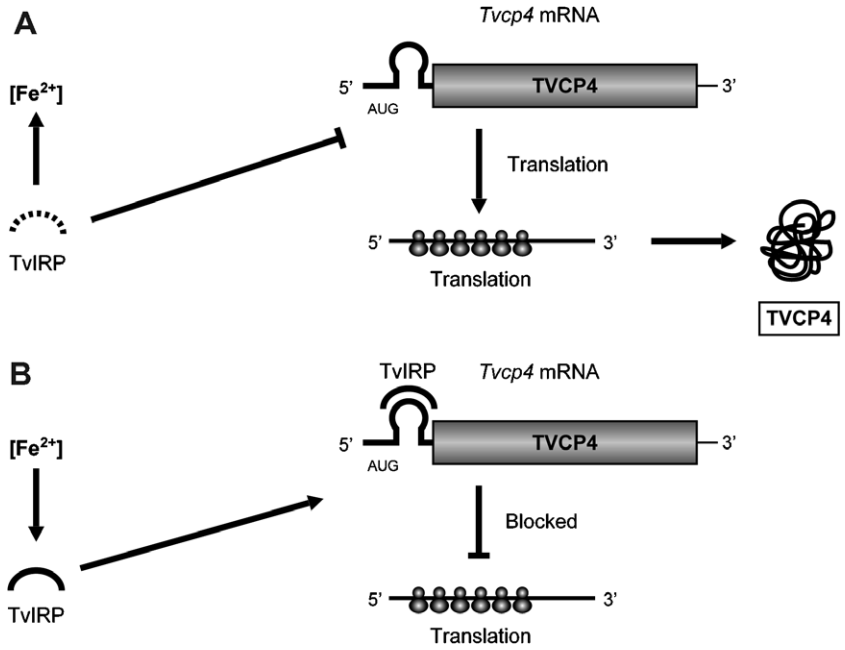

Fig. 6. A model to explain the post-transcriptional regulation of the *T. vaginalis tvcp4* gene expression by an IRE/IRP-like system. (A) At high-iron concentrations absence of IRP-like proteins (TvIRP) probably due to proteolytic degradation (dashed semicircle) will allow translation of the TVCP4 proteinase. (B) In low-iron concentrations presence of TvIRP-like proteins (semicircle) that bind to the IRE stem-loop structure of the *tvcp4* mRNA will block TVCP4 translation. Thus, TVCP4 will only be observed in trichomonad extracts of parasites grown at high iron concentrations, as shown in Fig. 1D.

region. This could be due to the short 5′-UTR promoter region in *T. vaginalis* genes [33], leaving the position of this IRE structure within the first 60-nt downstream of the cap structure, which is consistent with the position shown for iron upregulated genes in some mammalian cells [39,40].

Even though a decrease in translational efficiency with IREs located in coding regions has been documented only for artificial constructs thus far [39], it is noteworthy to mention that the IRE in the *tvcp4* mRNA is the first naturally found odd IRE in a gene that is positively regulated by iron at the protein synthesis level. Before this, the only lower organism in which an IRE-binding protein has been identified is *Plasmodium falciparum*, but even in that organism the identification of target mRNAs and post-transcriptional regulation is still somewhat hypothetical [41].

It is also interesting to note that the RNA–protein interactions results and competition data suggest that the *tvcp4* IRE structure has higher affinity for IRP proteins of HeLa cells than the IRE-fer itself. Thus, this odd IRE hairpin structure of *tvcp4* mRNA may represent a novel hairpin sequence found in natural mRNAs unrelated to iron homeostasis [14–17] that could be regulated by iron through RNA–protein interactions mediated by IRE/IRP-like systems, representing another stress signal as hypoxia, NO, and bacterial sporulation and motility, etc. [14–17,42].

The IRE structure of TVCP4 identified here has an unusual stem- and loop-sequence that has not been identified in any other iron-regulated IRE. Yet, all well documented cases of IRP-1 and IRP-2 regulated mRNAs in animal species have a rather tight consensus sequence. Only *in vitro* IRE mutants isolated by the SELEX technology with some odd sequences were shown to bind to IRPs, but none of these mutants were documented in regulated mRNAs of mammalian species. SELEX never selected any IRE with a C in position 3 of the loop as is the case with the TVCP4 IRE [28,29]. Our results suggest that we have found a post-transcriptional iron regulation through an IRE/IRP-like system in *T. vaginalis*. Therefore, we would expect to find differences in the trichomonad IRP-like protein sequence in addition to those found with IRE structures. Work is in progress to identify and characterize IRP-like proteins in *T. vaginalis*.

Our results suggest that IRE/IRP interaction is relevant to control translation of mRNA regulated by iron, as occurs with the ferritin gene [14–17]. For *T. vaginalis*, binding of an IRP-like protein to the novel IRE stem-loop structure identified in the *tvcp4* transcript suggests the existence of a post-transcriptional iron regulation mechanism. Our model suggests that at high iron, an IRP-like protein is absent; permitting no IRE/IRP interaction and allowing the *tvcp4* mRNA to be translated for increased amounts of TVCP4 (Fig. 6). This model is consistent with our experimental data and supports the existence of an alternative iron regulatory system in *T. vaginalis*. This is consistent with the insect SDHb, mammalian mitochondrial aconitase, 75-kDa subunit of the mitochondrial complex I, and Alzheimer's amyloidal precursor protein genes [43–45]. To our knowledge, this is the first time that an IRE/IRP-like iron regulatory system is identified in trichomonads and in protozoa.

Acknowledgments: This work was partially supported by Grants 33044-M and 43763-Q (to R.A.), and 40387-Z (to J.O.L.) from the Consejo Nacional de Ciencia y Tecnología (CONACyT), México. E.S.G. was a scholarship recipient also from CONACyT. We are grateful to Dr. Lucas Kühn from the Swiss Institute for Experimental Cancer Research (ISREC) for his kind donation of the pSPT-fer and pGEX-hIRP plasmids used as controls in this study. We also thank Dr. Esther Orozco and Jaime Ortega-Arroyo for critical review and

for proofreading the manuscript, respectively, and to Alfredo Padilla for his help with the artwork. Nancy Mena, Alberto García, and David González are acknowledged for their technical assistance.

References

[1] Wilson, M.E. and Britigan, B.E. (1998) Iron acquisition by parasitic protozoa. Parasitol. Today 14, 348–353.
[2] Gorrell, T.E. (1985) Effects of culture medium content on the biochemical composition and metabolism of *Trichomonas vaginalis*. J. Bacteriol. 161, 1228–1230.
[3] De Jesus, J.B., Ferreira, M.A., Cuervo, P., Britto, C., Silva-Filho, F.C. and Meyer-Fernandes, J.R. (2006) Iron modulates ecto-phosphohydrolase activities in pathogenic trichomonads. Parasitol. Int. 55, 285–290.
[4] Lehker, M.W., Arroyo, R. and Alderete, J.F. (1991) The regulation by iron of the synthesis of adhesins and cytoadherence levels in the protozoan *Trichomonas vaginalis*. J. Exp. Med. 174, 311–318.
[5] Arroyo, R., Engbring, J., Nguyen, J., Musatovova, O., Lopez, O., Lauriano, C. and Alderete, J.F. (1995) Characterization of cDNAs encoding adhesin proteins involved in *Trichomonas vaginalis* cytoadherence. Arch. Med. Res. 26, 361–369.
[6] Garcia, A., Chang, T., Benchimol, M., Klumpp, D., Lehker, M. and Alderete, J.F. (2003) Iron and contact with host cells induce expression of adhesins on surface of *Trichomonas vaginalis*. Mol. Microbiol. 47, 1207–1224.
[7] Moreno-Brito, V., Yañez-Gómez, C., Meza-Cervántez, P., Avila-González, L., Rodríguez-Rodríguez, M.A., Ortega-López, J., González-Robles, A. and Arroyo, R. (2005) A *Trichomonas vaginalis* 120-kDa protein with identity to hydrogenosome pyruvate ferredoxin oxidorreductase is a surface adhesin induced by iron. Cell. Microbiol. 7, 245–258.
[8] Alderete, J.F., Provenzano, D. and Lehker, M.W. (1995) Iron mediates *Trichomonas vaginalis* resistance to complement lysis. Microb. Pathogen. 19, 93–103.
[9] Crouch, M.L. and Alderete, J.F. (2001) *Trichomonas vaginalis* has two fibronectin-like iron-regulated genes. Arch. Med. Res. 32, 102–107.
[10] León-Sicairos, C.R., León-Félix, J. and Arroyo, R. (2004) *Tvcp12*: a novel *Trichomonas vaginalis* cathepsin L-like cysteine proteinase-encoding gene. Microbiology (UK) 150, 1131–1138.
[11] Tsai, C.D., Liu, H.W. and Tai, J.H. (2002) Characterization of an iron-responsive promoter in the protozoan pathogen *Trichomonas vaginalis*. J. Biol. Chem. 277, 5153–5162.
[12] Ong, S.J., Huang, S.C., Liu, H.W. and Tai, J.S. (2004) Involvement of multiple DNA elements in iron-inducible transcription of the *ap65-1* gene in the protozoan parasite *Trichomonas vaginalis*. Mol. Microbiol. 52, 1721–1730.
[13] Ong, S.J., Hsu, H.M., Liu, H.W., Chu, C.H. and Tai, J.H. (2007) Activation of multifarious transcription of an adhesion protein *ap65-1* gene by a novel Myb2 protein in the protozoan parasite *Trichomonas vaginalis*. J. Biol. Chem. 282, 6716–6725.
[14] Testa, U. (2002) Iron-responsive elements and iron regulatory proteins in: Proteins of Iron Metabolism (Testa, U., Ed.), pp. 407–448, CRC Press, Boca Raton, FL, USA.
[15] Pantopoulos, K. (2004) Iron metabolism and the IRE/IRP regulatory system. Ann. N. Y. Acad. Sci. 1012, 1–13.
[16] Hentze, M.W., Muckenthaler, M.U. and Andrews, N.C. (2004) Balancing acts: molecular control of mammalian iron metabolism. Cell 117, 285–297.
[17] Rouault, T.A. (2006) The role of iron regulatory proteins in mammalian iron homeostasis and disease. Nat. Chem. Biol. 2, 406–414.
[18] Neale, K.A. and Alderete, J.F. (1990) Analysis of the proteinases of representative *Trichomonas vaginalis* isolates. Infect. Immun. 58, 157–162.
[19] Arroyo, R. and Alderete, J.F. (1989) *Trichomonas vaginalis* surface proteinase activity is necessary for parasite adherence to epithelial cells. Infect. Immun. 57, 2991–2997.
[20] Mendoza-López, R., Becerril-García, C., Fattel-Facenda, L.V., Avila- González, L., Ruiz-Tachiquín, M., Ortega-López, J. and Arroyo, R. (2000) CP30, a cysteine proteinase involved in *Trichomonas vaginalis* cytoadherence. Infect. Immun. 68, 4907–4912.
[21] Hernandez, H., Sariego, I., Garber, G., Delgado, R., Lopez, O. and Sarracent, J. (2004) Monoclonal antibodies against a 62 kDa proteinase of *Trichomonas vaginalis* decrease parasites cytoadherence to epithelial cells and confer protection to mice. Parasite Immunol. 26, 119–125.
[22] Alvarez-Sánchez, M.E., Avila-González, L., Becerril-García, C., Fattel-Facenda, L.V. and Arroyo, R. (2000) A novel cysteine proteinase (CP65) of *Trichomonas vaginalis* involved in cytotoxicity. Microb. Pathog. 28, 193–202.
[23] Hernández-Gutiérrez, R., Avila-González, L., Ortega-López, J., Cruz-Talonia, F., Gómez-Gutiérrez, G. and Arroyo, R. (2004) *Trichomonas vaginalis*: characterization of a 39-kDa cysteine proteinase found in patient vaginal secretions. Exp. Parasitol. 107, 125–135.
[24] Diamond, L. (1957) The establishment of various trichomonads of animals and men in axenic culture. J. Parasitol. 43, 488–490.
[25] Zuker, M. (2003) Mfold web server for nucleic acid folding and hybridization prediction. Nucleic Acids Res. 31, 3406–3415.
[26] Alderete, J.F. (1983) Antigenic analysis of several pathogenic strains of *Trichomonas vaginalis*. Infect. Immun. 39, 1041–1047.
[27] Kaldy, P., Menotti, E., Moret, R. and Kühn, L.C. (1999) Identification of RNA-binding surfaces in iron regulatory protein-1. EMBO J. 18, 6073–6083.
[28] Henderson, B.R., Menotti, E., Bonard, C. and Kühn, L.C. (1994) Optimal sequence and structure of iron-responsive elements. Selection of RNA-stem-loops with high affinity for iron regulatory factor. J. Biol. Chem. 269, 17481–17489.
[29] Henderson, B.R., Menotti, E. and Kühn, L.C. (1996) Iron regulatory proteins 1 and 2 bind distinct sets of RNA target sequences. J. Biol. Chem. 271, 4900–4908.
[30] Harlow, D. and Lane, E. (1988) Antibodies: A Laboratory Manual, Cold Spring Harbor Laboratory, New York, USA.
[31] Campbell, K.S., Bedzyk, W.D. and Cambier, J.C. (1995) Manipulation of B cell antigen receptor tyrosine phosphorylation using aluminum fluoride and sodium orthovanadate. Mol. Immunol. 32, 1283–1294.
[32] Gutierrez-Escolano, L., Vazquez-Ochoa, M., Escobar-Herrera, J. and Hernandez-Acosta, J. (2003) La, PTB, and PAB proteins bind to the 3′ untranslated region of Norwalk virus genomic RNA. Biochem. Biophys. Res. Commun. 311, 759–766.
[33] Liston, D.R. and Johnson, P.J. (1999) Analysis of a ubiquitous promoter element in a primitive eukaryote: early evolution of the initiator element. Mol. Cell. Biol. 19, 2380–2388.
[34] Espinosa, N., Hernández, R., López-Griego, L., Arroyo, R. and López-Villaseñor, I. (2001) Differences between coding and non-coding regions in the *Trichomonas vaginalis* genome: an actin gene as a locus model. Acta Trop. 78, 147–154.
[35] Mallinson, D.J., Lockwood, B.C., Coombs, G.H. and North, M. (1994) Identification and molecular cloning of four cysteine proteinase genes from the pathogenic protozoan *Trichomonas vaginalis*. Microbiology 140, 2725–2735.
[36] Carlton, J.M., Hirt, R.P., Silva, J.C., Delcher, A.L., Schatz, M., et al. (2007) Draft genome sequence of the sexually transmitted pathogen *Trichomonas vaginalis*. Science 315, 207–212.
[37] Addess, K.J., Basilion, J.P., Klausner, R.D., Rouault, T.A. and Pardi, A.J. (1997) Structure and dynamics of the iron responsive element RNA: implications for binding of the RNA by iron regulatory proteins. J. Mol. Biol. 274, 72–83.
[38] Lin, E., Graziano, J.H. and Freyer, G.A. (2001) Regulation of the 75-kDa subunit of mitochondrial complex I by iron. J. Biol. Chem. 276, 27685–27692.
[39] Paraskeva, E., Gray, N.K., Schläger, B., Wehr, K. and Hentze, M.W. (1999) Ribosomal pausing and scanning arrest as mechanisms of translational regulation from cap-distal iron-responsive elements. Mol. Cell. Biol. 19, 807–816.
[40] Koloteva, N., Mueller, P.P. and McCarthy, J.E.G. (1997) The position dependence of translational regulation via RNA–RNA and RNA–protein interactions in the 5′-untranslated region. J. Biol. Chem. 271, 16531–16539.
[41] Loyevsky, M., Mompoint, F., Yikilmaz, E., Altschul, S.F., Madden, T., Wootton, J.C., Kurantsin-Mills, J., Kassim, O.O., Gordeuk, V.R. and Rouault, T.A. (2003) Expression of a recombinant IRP-like *Plasmodium falciparum* protein that

specifically binds putative plasmodial IREs. Mol. Biochem. Parasitol. 126, 231–238.
[42] Serio, A.W., Pechter, K.B. and Sonenshein, A.L. (2006) *Bacillus subtilis* aconitase is required for efficient late-sporulation gene expression. J. Bacteriol. 188, 6396–6405.
[43] Rogers, J.T., Randall, J.D., Cahill, C.M., Eder, P.S., Huang, X., Gunshin, H., Leiter, L., McPhee, J., Sarang, S.S., Utsuki, T., Greig, N.H., Lahiri, D.K., Tanzi, R.E., Bush, A.I., Giordano, T. and Gullans, S.R. (2002) An iron-responsive element type II in the 5′-untranslated region of the Alzheimer's amyloid precursor protein transcript. J. Biol. Chem. 277, 45518–45528.
[44] Kohler, S.A., Henderson, B.R. and Kühn, L.C. (1995) Succinate dehydrogenase b mRNA of *Drosophila melanogaster* has a functional iron-responsive element in its 5′-untranslated region. J. Biol. Chem. 270, 30781–30786.
[45] Kim, H.Y., LaVaute, T., Iwai, K., Klausner, R.D. and Rouault, T.A. (1996) Identification of a conserved and functional iron-responsive element in the 5′-untranslated region of mammalian mitochondrial aconitase. J. Biol. Chem. 271, 24226–24230.